



Microporous Development in Cashew Branch Activated Carbon: Comparative Effects of Sodium and Potassium Hydroxides

Konan Gbangbo Rémis¹, Dongo Koffi René², Ehouman Ahissan Donatien³,
Diarrassouba Aïcha Samira³

¹Laboratory of Geographical Sciences, Civil Engineering and Geosciences (LASCIG3) of the Joint Research and Innovation Unit for Engineering Sciences and Techniques (UMRI-STI) of the Institut National Polytechnique Félix HOUPHOUËT-BOIGNY (INP-HB), BP 1093 Yamoussoukro, Côte d'Ivoire.

²Laboratory of Industrial Processes and Synthesis of the Environment and New Energies, of the Institut National Polytechnique Félix HOUPHOUËT-BOIGNY (INP-HB), BP 1093 Yamoussoukro, Côte d'Ivoire.

³Laboratory of Thermodynamics and Physico-Chemistry of the Environment (LTPCM), UFR Applied Fundamental Sciences, Nangui Abrogoua University, Abidjan, P.O. Box 801, Abidjan 02, Côte d'Ivoire
Corresponding author email: konanremis@gmail.com

<http://dx.doi.org/10.13005/ojc/420131>

Received : 30-Dec-2025; Accepted : 13-Feb-2026

ABSTRACT

Chemical activation of lignocellulosic biomass is a cost effective route to tailor microporosity in activated carbons (ACs) for adsorption and gas purification. This study evaluates the comparative effects of sodium hydroxide (NaOH) and potassium hydroxide (KOH) on the development of microporosity in activated carbon derived from cashew (*Anacardium occidentale*) branch biomass. The precursor was size reduced, sieved (pass at 8 mm; retain at 4 mm), impregnated for 24 h in alkaline solutions (typically 500 ppm), oven dried (24 h), carbonized in lidded porcelain containers at 500 °C for 3h10 (NaOH) or 3 h 00 (KOH), and subsequently washed to near neutral pH and re dried. Yield was quantified by mass balance. Microporosity was assessed using the iodine number test (0.1 N I₂, titration with 0.1 N Na₂S₂O₃, starch indicator), a well established proxy for the presence of small pores in ACs. Under the stated conditions, average production yields were ~35%. The iodine numbers obtained were ~533 mg•g⁻¹ for NaOH activated samples and ~571 mg•g⁻¹ for KOH activated samples at 500 °C, indicating a modest advantage of KOH in creating/expanding micropores in this feedstock. Overall, activation agent, impregnation ratio, and thermal schedule critically determine micropore development; KOH shows slightly higher efficacy than NaOH in the present cashew branch system. The results support the viability of cashew branch biomass as a local, sustainable precursor for microporous AC production.

Keywords: Activated carbon; cashew branch biomass; NaOH; KOH; chemical activation; microporosity; iodine number; impregnation; pyrolysis.



INTRODUCTION

Activated carbon (AC) produced from lignocellulosic biomass is widely employed for the removal of pollutants and trace contaminants^[1, 2, 3] due to its high surface area and tunable pore texture^[4, 5]. Microporosity (pore width < 2 nm) is a decisive contributor to adsorption capacity for small molecules and many gaseous contaminants. Chemical activation—especially with strong bases (NaOH, KOH)—is frequently used to enhance pore development at relatively moderate temperatures, by promoting dehydration, aromatization, and mineral templated etching of the carbon matrix during pyrolysis^[4, 6, 7, 8]. The cashew tree (*Anacardium occidentale*) is abundant in West Africa. Cashew branch biomass represents an underutilized residue that can be valorized into AC, supporting circular economy goals. In practice, the iodine number is a rapid, standardized indicator of AC microporosity and a proxy for surface area associated with small pores; values $\geq 500 \text{ mg}\cdot\text{g}^{-1}$ are commonly interpreted as evidence of significant microporous character in many application contexts. Chemical activation with NaOH/KOH is known to intercalate and react with the char matrix, creating pores through gas evolution and mineral removal upon washing, whereas the extent of micropore development depends on impregnation ratio, activation temperature/time, and post treatment. The selected precursor, cashew branch biomass, has not been reported in the literature so far, unlike the more commonly studied cashew shells or agricultural residues. The distinct lignocellulosic composition and mineral profile of cashew branch biomass justify a dedicated investigation of its response to alkaline activation because the chemical architecture of lignocellulose—particularly the proportions and structural organization of cellulose, hemicellulose, and lignin—varies significantly among plant species and organs, strongly influencing thermal decomposition and activation chemistry [16]. Wood and branch tissues also exhibit highly variable inorganic ash contents rich in Ca, Mg, K, and other minerals that serve as natural catalysts and templates during carbonization, thereby altering pore development mechanisms^[17]. Moreover, recent studies have demonstrated that ionic properties of alkaline reagents interact differently with lignocellulosic substrates depending on their intrinsic mineral profiles, leading to distinct

degrees of disruption and heterogeneous activation behaviors between NaOH and KOH^[18]. Additional work on chemical activation of lignocellulosic precursors further shows that precursor composition critically governs impregnation efficiency, reagent penetration, lignin removal, and the resulting porosity, reinforcing the necessity of evaluating cashew branch biomass as a distinct raw material^[5]. This work compares NaOH and KOH activation routes applied to cashew branch precursor under controlled laboratory conditions and quantifies their effect on microporosity via iodine number.

MATERIALS AND METHODS

Equipment and Supplies

A comprehensive suite of laboratory equipment and materials was employed to ensure rigorous control over each stage of precursor preparation, chemical activation, and physicochemical evaluation. Initial size reduction of the cashew branch feedstock was performed manually using a wooden mortar and pestle, enabling gentle comminution while preserving the structural integrity of the lignocellulosic fragments prior to classification. Particle homogenization was achieved through mechanical sieving using 8 mm and 4 mm mesh sizes, thereby isolating a controlled granulometric fraction suitable for reproducible impregnation and thermal processing. Chemical activation was initiated by immersing the sieved precursor in alkaline solutions contained within seal tight glass jars, which prevented evaporative losses and ensured consistent solid–liquid contact during impregnation. Pre and post treatment dehydration steps were conducted in a precision regulated drying oven, whereas carbonization occurred in a high temperature electric furnace, where porcelain crucibles and containers provided inert, thermally stable vessels capable of withstanding the pyrolytic environment. To limit parasitic oxidation and maintain a quasi oxygen limited atmosphere during pyrolysis, paper covers were applied over crucible lids, promoting controlled devolatilization rather than oxidative degradation. After carbonization, the resulting chars underwent repeated aqueous washing with distilled water, during which the effluent pH was continuously monitored using a calibrated pH meter to ensure the complete removal of residual alkaline species and soluble mineral fractions. Mass

measurements at all critical stages—raw biomass, impregnated precursor, carbonized product, and washed carbon—were performed using analytical and top loading balances to ensure high precision yield determination. The cleaned and oven dried activated carbons were subsequently stored in airtight plastic containers, preventing rehydration or atmospheric contamination prior to characterization. Microporosity assessment by the iodine number method required burettes, Erlenmeyer flasks, beakers, and a laboratory stopwatch, alongside magnetic stirrers to guarantee homogeneous mixing during titrimetric analyses. Throughout all experimental procedures, strict adherence to laboratory safety protocols was maintained by consistently employing personal protective equipment (PPE), including lab coats, safety glasses, gloves, and dust masks, thereby ensuring safe handling of chemical reagents, hot materials, and fine particulate matter.

Precursor Preparation

Branches of cashew were cut into twigs of approximately 5 cm length, air dried, and mechanically size reduced in a wooden mortar and pestle. The reduced material was sieved; fractions passing 8 mm and retained at 4 mm were selected and stored in clean containers for subsequent



Figure 1: Raw material (left) and Sieve (right)

Activating Solutions and Impregnation

Impregnation ratios and activation conditions were selected based on previous optimization studies^[9]. Activating solutions of NaOH and KOH were prepared at specified concentrations of 500 ppm:

- For 500 ppm: dissolve 0.5 g of reagent in distilled water and bring to a final volume of 1,000 mL.

The activation procedure follows approaches reported for lignocellulosic biomass^[10, 11].

The impregnation ratio was 15 g precursor per 50

mL of activating solution. The precursor was placed in glass jars with lids, ensuring complete immersion of solids. Impregnation time was 24 hours, followed by oven drying for 24 h (to remove unbound moisture prior to carbonization).

Carbonization (Pyrolysis)

Impregnated and oven dried precursors were transferred into porcelain containers and covered to reduce oxygen ingress, then placed in a muffle furnace at:

- 500 °C for 3 h 10 (NaOH)
- 500 °C for 3 h 00 (KOH)

After carbonization, hot samples were allowed to cool inside the furnace or in ambient air under covered conditions.

Washing and Post Drying

Carbonized materials were washed repeatedly with distilled water until the pH of the rinsate approached 7, indicating the removal of residual alkaline species and soluble ash. Washed carbons were oven dried for 24 h and stored in sealed containers pending characterization.

Yield Determination

The production yield R was determined gravimetrically:

$$R (\%) = [(m_1 / m_0)] \times 100$$

where m_0 is the initial mass of impregnated precursor and m_1 is the mass of the corresponding carbonized product.

Iodine Number Determination (Microporosity Proxy)

Microporosity was assessed via the iodine number using titration:

- Weigh 0.050 g of activated carbon into a 100 mL beaker.
- Add 15 mL of 0.1 N iodine (I_2) solution.
- Agitate for 5 min and filter to obtain the filtrate.
- Pipette 10 mL of the filtrate into an Erlenmeyer.
- Titrate with 0.1 N sodium thiosulfate ($Na_2S_2O_3$) to a colorless endpoint using starch (≈ 3 drops) as indicator.

A blank (without adsorbent) was run under identical conditions; the blank thiosulfate volume was $V_b=5.4$ mL. V_s : the thiosulfate volume for the sample filtrate.

The iodine number (I_d , $mg \cdot g^{-1}$) was computed as:

$$\text{Iodine index (mg/g)} = \frac{(V_b - V_s) \cdot N \cdot 126.9 \cdot 1.5}{M}$$

where N is the normality of $\text{Na}_2\text{S}_2\text{O}_3$ (0.1 N), 126.9 is the atomic mass of iodine ($\text{mg} \cdot \text{mmol}^{-1}$), the factor 1.5 accounts for the ratio of initial iodine volume (15

mL) to the 10 mL aliquot titrated, and M is the mass of adsorbent (g), here 0.050 g (Figure 2).



Figure 2: Balance

RESULTS

Carbonization Yield

The two carbonization tests conducted at 500 °C yielded consistent results, with values of 36.66 % and 35.30 %, corresponding to an average of approximately 36 % and a relative standard deviation of about 2.7 %. This low variability indicates good reproducibility of the process under the specified conditions (covered porcelain containers, 3 h–3 h 10 dwell time). The slight difference of 1.36 percentage points between tests is attributable to minor factors such as residual moisture or handling losses, rather than any significant process deviation. These yields align closely with the overall

study average (~35 %), confirming that the 500 °C protocol provides stable conversion of cashew branch biomass into activated carbon. However, it is important to note that yield alone does not reflect microporosity development; despite similar yields, KOH activation at this temperature produced higher iodine numbers than NaOH, underscoring those textural properties depend more on activation chemistry and thermal schedule than on mass retention.

Iodine Number (Microporosity Indicator)

Under the impregnation conditions (500 ppm, 15 g/50 mL, 24 h), the iodine numbers measured for NaOH and KOH at 500 °C are summarised in Table 1:

Table 1: Iodine index values

Impregnation		Iodine index		
Activation agent	Concentration	Impregnation ratio	Impregnation time	Io (mg/g)
NaOH	500ppm	15g/50ml	24h	532.98
KOH	500ppm	15g/50ml	24h	571.05

Analysis and Discussion

Yield and Process Efficiency

The ~35% yield observed is consistent with thermal removal of volatiles and the conversion of lignocellulosic matter to a more carbon rich, porous matrix during pyrolysis. Differences among tests reflect variations in initial mass, heating schedule, and laboratory setup. Covered porcelain containers and paper seals likely contributed to limiting oxygen ingress, favoring pyrolytic (rather than oxidative) pathways and preserving carbon yield.

Microporosity Development: NaOH vs KOH

The measured iodine values indicate that both NaOH and KOH activation successfully generated microporous structures in ACs derived from cashew branches, with KOH producing higher values under otherwise comparable conditions (571 $\text{mg} \cdot \text{g}^{-1}$ vs ~533 $\text{mg} \cdot \text{g}^{-1}$ at 500 °C) (Figure 3). This modest but consistent advantage aligns with widely reported mechanisms in alkaline activation of biomass derived carbons: KOH tends to intercalate more effectively, promote gas evolution (e.g., H_2 , CO, CO_2 through redox reactions with carbon/oxygen complexes)

[12, 13], and facilitate etching that opens and widens micropores [8].

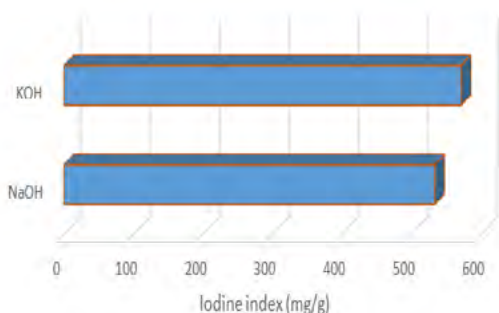


Figure 3: Iodine index comparison (KOH vs NaOH)

Impregnation Ratio, Residence Time, and Thermal Schedule

Consistent with prior literature, the impregnation ratio (mass of activating agent solution per mass of precursor), treatment times (impregnation, carbonization), and carbonization temperature significantly affect the formation and widening of micropores. Increasing impregnation ratio generally enhances micropore density up to an optimum [7, 9] beyond which pore widening or wall degradation can reduce the iodine number [14, 7]. Similarly, longer dwell times at a given temperature can improve porosity until over activation decreases structural integrity and micropore fidelity [15].

In comparison with published values for similar lignocellulosic precursors, the iodine numbers obtained in this study ($\approx 533 \text{ mg}\cdot\text{g}^{-1}$ for NaOH and $\approx 571 \text{ mg}\cdot\text{g}^{-1}$ for KOH at 500°C) fall clearly within the typical range reported for agricultural residue based activated carbons, generally between 500 and $650 \text{ mg}\cdot\text{g}^{-1}$ depending on activation conditions. For example, Tan et al. [19] and Danish & Ahmad [2] report comparable microporosity values for activated carbons derived from wood and agro forest residues, while Yahya et al. [3] situate most alkali activated carbons within this same interval. The moderately higher performance observed for KOH in our system is also consistent with the mechanisms described by Zhang et al. [4], who show that KOH activation involves (i) more efficient intercalation of K ions into the carbon matrix, (ii) formation of potassium carbonate and metallic potassium, (iii) substantial gas evolution (H_2 , CO , CO_2) contributing to pore opening, and (iv) stronger etching of the carbon framework that widens micropores. NaOH proceeds through similar mechanisms but with lower ionic mobility and

reduced intercalation capability, typically yielding slightly lower micropore development under identical conditions. Overall, activated carbons derived from cashew branch biomass position themselves well within the performance range commonly reported for lignocellulosic activated carbons, confirming the relevance of this local residue as a viable precursor for producing microporous materials comparable to those obtained from more extensively studied biomass sources.

CONCLUSION

Activated carbons produced from cashew branch biomass via alkaline chemical activation demonstrate meaningful microporosity, with KOH showing a slight advantage over NaOH under comparable conditions. Iodine numbers around $571 \text{ mg}\cdot\text{g}^{-1}$ (KOH) and $533 \text{ mg}\cdot\text{g}^{-1}$ (NaOH) at 500°C confirm the feasibility of this local biomass for microporous AC production and support its sustainable valorization. Careful optimization of alkaline activation (ratio, temperature, time) can further improve outcomes without the drawbacks associated with strong acidic processing. Future work should incorporate systematic parametric studies (impregnation ratios, multi step thermal programs), comprehensive textural characterization (BET surface area, pore size distribution via N adsorption at 77 K), and application oriented testing (e.g., biogas cleaning, water treatment) to fully exploit the potential of cashew branch derived AC.

Limitations and Future Work

- The present characterization relies on the iodine number as a fast microporosity proxy. Additional analyses (BET, BJH/DFT pore size distributions, ash content, elemental analysis, SEM) are recommended to map the full textural and chemical landscape.
- The drying temperature during oven steps and the atmosphere during carbonization were not rigorously controlled beyond covered porcelain setups; future runs should consider inert gas purging to improve reproducibility.
- Impregnation ratios and solution concentrations should be varied systematically (including ≥ 500 ppm and higher solid/liquid ratios) to identify operating optima.
- Kinetic studies (time dependent iodine adsorption) and regeneration performance would

strengthen application relevance.

ACKNOWLEDGMENTS

The authors thank the Laboratory of Geographical Sciences, Civil Engineering and Geosciences and Laboratory of Industrial Processes and Synthesis of the Environment and New Energies and the Laboratory of Thermodynamics and Physico-Chemistry of the Environment for access to furnaces and analytical equipment and acknowledge the assistance of laboratory staff during carbonization and titrimetric analyses.

Conflicts of Interest

The authors declare no conflicts of interest.

Data Availability statement

All data generated or analyzed during this study are available from the corresponding author

upon reasonable request.

Funding Source Statement

This research was funded by the authors' own resources and institutional support from the Institut National Polytechnique Félix Houphouët-Boigny (INP-HB), Côte d'Ivoire. No external funding was received for this study.

Ethical Approval Statement

This study did not involve human participants or animal subjects; therefore, ethical approval was not required.

Informed Consent Statement

Not applicable. No human participants were involved in this research.

REFERENCES

1. X.F. Tan, S.B. Liu, Y.G. Liu, Y.L. Gu, G.M. Zeng, X.J. Hu, X. Wang, S.H. Liu and L.H. Jiang, *Bioresour. Technol.*, **2017**, 227, 359–372.
2. M. Danish and T. Ahmad, *Renew. Sustain. Energy Rev.*, **2018**, 87, 1–21.
3. M.A. Yahya, Z. Al-Qodah and C.W.Z. Ngah, *Renew. Sustain. Energy Rev.*, **2015**, 46, 218–235.
4. C. Zhang, S. Sun, S. He and C. Wu, *J. Energy Inst.*, **2022**, 105, 399–405.
5. J. Alcañiz-Monge, M.D.C. Román-Martínez and M.Á. Lillo-Ródenas, *Molecules*, **2022**, 27(5), 1630.
6. D. Kumari and R. Singh, *Renew. Sustain. Energy Rev.*, **2018**, 90, 877–891.
7. M.J. Ahmed and S.K. Dhedan, *Fluid Phase Equilibria*, **2012**, 317, 9–14.
8. N.A. Rashidi and S. Yusup, *Environ. Sci. Pollut. Res.*, **2019**, 26(33), 33732–33746.
9. A. Ronix, *J. Environ. Chem. Eng.*, **2017**, 5(5), 4841–4849.
10. N. Mohamad Nor, L.C. Lau, K.T. Lee and A.R. Mohamed, *J. Environ. Chem. Eng.*, **2013**, 1(4), 658–666.
11. M.S. Shafeeyan, W.M.A.W. Daud, A. Houshmand and A. Shamiri, *J. Anal. Appl. Pyrolysis*, **2010**, 89(2), 143–151.
12. W. Fan, A. Chakraborty and S. Kayal, *Energy*, **2016**, 102, 491–501.
13. J. Gopalan, A. Buthiyappan and A.A. Abdul Raman, *J. Ind. Eng. Chem.*, **2022**, 113, 72–95.
14. W. Tongpoothorn, M. Sriuttha, P. Homchan, S. Chanthai and C. Ruangviriyachai, *Chem. Eng. Res. Des.*, **2011**, 89(3), 335–340.
15. G. Coppola and D. Papurello, *Clean Technol.*, **2018**, 1(1), 40–57.
16. T.A.L. Silva, L.H. Ribeiro Varão and D. Pasquini, *Lignocellulosic Biomass, Springer Nature*, **2023**.
17. R.C. Pettersen, "The Chemical Composition of Wood," *Springer archival chapter*, **1984**.
18. U. Shakeel, Y. Zhang, C. Liang, W. Wang and W. Qi, *Int. J. Biol. Macromol.*, **2024**.
19. X. Tan, S. Liu, Y. Liu, Y. Gu, G. Zeng, X. Hu, X. Wang, S. Liu and L. Jiang, *Bioresour. Technol.*, **2017**, 227, 359–372.